Smart Structures and Systems, *Vol. 24, No. 2 (2019) 257-266*
DOI: https://doi.org/10.12989/sss.2019.24.2.257

Data fusion based improved HOSM observer for smart structure control

J. Arunshankar*

Department of Instrumentation and Control Systems Engineering, PSG College of Technology, Coimbatore – 641 004, India

(Received February 7, 2017, Revised April 2, 2019, Accepted April 4, 2019)

Abstract. The benefit of data fusion in improving the performance of Higher Order Sliding Mode (HOSM) observer is brought out in this paper. This improvement in the performance of HOSM observer, resulted in the improvement of active vibration control of a piezo actuated structure, when controlled by a Discrete Sliding Mode Controller (DSMC). The structure is embedded with two piezo sensors for measuring the first two vibrating modes. The fused output of sensors is applied to the HOSM observer for generating state estimates, these states generated are applied to the DSMC, designed for the fourth order linear time invariant model of the structure. In the simulation study, the structure is excited at the first and second mode resonance. It is found that better vibration suppression is obtained, when the states generated by the fused output of sensors is applied as controller input, than the vibration suppression obtained by applying the states generated by using individual sensor output. The closed loop performance of DSMC obtained with HOSM observer is compared with the closed loop performance obtained with the conventional observer. Results obtained shows that better vibration suppression is obtained when the states generated by HOSM observer is applied as controller input.

Keywords: piezo actuated structure; data fusion; higher order sliding mode observer; discrete sliding mode controller

1. Introduction

A smart or adaptive structure can sense its dynamic loading environment using sensors and modify its behaviour in real time, so that it can withstand external dynamic forces, such as earthquake loading, wind or impact. Such a system consists of three components: sensors, actuators and a computer. The sensor measures the displacements along the degrees of freedom, the computer which hosts the control algorithm determines the magnitude of control forces appropriate to the uncontrolled response at any given time, and the actuator applies the required forces to compensate for the forces of nature and minimize the vibrations of the structure, is reported in Fisco and Adeli (2011), Hurlebaus (2006). Control techniques like LQR, LQG, robust H_2 and sliding mode control are applied for vibration control of smart structure systems.

Sliding Mode Control (SMC) is one of the most popular approaches to control nonlinear systems. Owing to the main reasons of high robustness, easy design and implementation, it is applied in large number of applications. The idea of SMC is to transfer a system to a state, from which it can be easily driven to the equilibrium state. SMC consists of two phases, in the first phase, the system approaches the sliding surface from the initial state called approaching phase and, in the second phase the system slides along the sliding surface to the final state called sliding phase. But due to the presence of model uncertainty and disturbances, the control law is discontinuous across the sliding surface. Since the associated control switching is represented by a signum function in the control law, undesirable chattering of control signal arises, is reported in Utkin (1992) and Petr Husek (2016).

SMC is applied for various control problems. Output feedback sliding mode control for sampled data systems in the presence of external disturbances is reported in Nguyen *et al.* (2016). Zhang *et al.* (2016) proposed a disturbance observer based integral sliding-mode control approach for continuous time linear systems with mismatched disturbances or uncertainties. An output feedback stabilization of perturbed double integrator system using supertwisting control is proposed by Chalanga *et al.* (2016). A novel adaptive terminal SMC for a steer-by-wire vehicle is proposed, and it is shown that the controller can drive the closed loop error dynamics to converge to zero in a finite time, with adaptive laws being applied to estimate the uncertain bounds of the system parameters and disturbances in Lyapunov sense, is reported in Wang *et al.* (2016).

SMC is applied extensively for smart structure control applications. Kim *et al.* (2013) proposed a new model predictive sliding mode control algorithm for active vibration suppression of a 1D piezoelectric bimorph structure, with model predictive control employed to enhance the performance of SMC, by enforcing the system to reach the sliding surface in an optimal manner. An adaptive fuzzy sliding mode based output control for magneto-rheological damper to suppress vibrations of the nonlinear structure is developed by Li *et al.* (2013). Hassani *et al.* (2010) developed a novel smart MEMS accelerometer which employs a SMC, added to a conventional PID closed loop system to achieve higher stability, higher dynamic

*Corresponding author, Professor
E-mail: j_arunshankar@yahoo.com

http://www.techno-press.com/journals/sss&subpage=7 ISSN: 1738-1584 (Print), 1738-1991 (Online)

range and to prevent pull-in phenomena by preventing finger displacement from passing a maximum preset value, as well as added an adaptive nonlinear observer to a conventional PID closed loop system, which resulted in better resolution. Precision motion control of a piezoelectric nanopositioning stage using a new adaptive SMC, with uncertainty and disturbance estimation, inherent chattering free control action guaranteed by eliminating the use of discontinuous control term is proposed by Xu (2017). SMC to suppress the hysteresis nonlinearity of the piezo actuated stages is proposed by Xu and Zhou (2017).

In the earliest work by Utkin, where SMC is applied for state estimation, utilizes a discontinuous switched component within an observer. Sliding Mode Observers (SMO) is widely used due to the finite-time convergence, robustness with respect to uncertainties and the possibility of uncertainty estimation, is reported in Utkin (1992). Application of SMO for fault detection and isolation is reported in Edwards *et al.* (2000). In HOSM observer, chattering effect which is inherent in the classical first order SMO and SMC is minimised. It generalises the basic sliding mode idea of, acting on the higher order time derivatives of the system deviation from the constraint, instead of influencing the first deviation derivative as it happens in standard sliding modes, is reported in Fridman and Levant (2002). HOSM observer, for detection of actuator faults is proposed by Capisani *et al.* (2012). Speed estimation of sensorless induction motor drives based on second order sliding mode supertwisting algorithm and Model Reference Adaptive System (MRAS) estimation theory, with variations of stator resistance and rotor resistance is reported in Zhao *et al.* (2014).

Data fusion is the process of combining output from sensors, with information from other sensors, information processing blocks, databases or knowledge bases, into one representational form. This technique is expected to achieve improved accuracy and more specific inferences than could be achieved by the use of a single sensor, as reported in Mutambara (1998) and James Linas (2008). Kalman filter based algorithms have been proposed for multisensor data fusion for both military and civilian applications.

The two broad classifications of data fusion techniques are state vector fusion and measurement fusion, in which there are two methods in state vector fusion. In the first method, the states are separately and parallelly estimated from sensor output, and then fused in a central processor to obtain an improved state estimate. In the second method, states estimated from first sensor acts as initial state for the second sensor, and the complete sensors array work in cascade fashion. In measurement fusion, a single state estimator incorporates all the weighted or combined measurements to obtain a single state estimate. Comparatively, the performance of measurement fusion technique is better than state vector fusion, but when it comes to flexibility and computational efficiency, state vector fusion outperforms measurement fusion, as reported in Bierman and Belzer (1985), Gan and Harris (2001).

Application of data fusion for smart structure systems is reported in the literature. Dynamic displacement estimated with high accuracy by blending high sampling rate acceleration data with low sampling rate displacement measurement, using a two stage Kalman estimator, is reported in Kim *et al.* (2016). An extension of classical Kalman filter proposed for real time estimation of structural state and unknown inputs without using collocated acceleration measurements, is reported by Lei *et al.* (2016). Further data fusion of acceleration and displacement or strain measurements is used to prevent the drifts in the identified structural state and unknown inputs in real time. An extension of the classical Kalman filter for real time joint estimation of structural states and the unknown inputs, by fusing the data of partially measured displacement and acceleration responses to prevent the drifts, is proposed by Liu *et al.* (2016). A response estimation technique based on the Kalman state estimator applied for the structural health monitoring of a simply supported beam, which estimates the strain responses at unmeasured locations delivered highest performance by fusing acceleration, strain and tilt, by minimizing the intrinsic measurement noise, under non zero mean input excitations is reported in Palanisamy *et al.* (2015). Control of a piezo actuated structure using SMC with multisensor data fusion is reported in Arunshankar *et al.* (2011). Experimental investigation of the closed loop performance of discrete sliding mode controller with data fusion applied for the control of piezo actuated structure, which resulted in improved vibration suppression is reported in Arunshankar *et al.* (2013). Simultaneous stabilization of piezo actuated structures using fast output sampling control involving data fusion is reported in Arunshankar and Umapathy (2015).

In this work, a simulation study is carried out for the active vibration control of the smart structure system considered using DSMC. Output of two piezo sensors which measures vibration are fused, and applied to HOSM observer for generating states. The states generated by the observer are then applied to the controller, for performing control. Data fusion applied for improving the performance of HOSM observer is not reported in literature. The main contribution of this work is to improve the performance of HOSM observer, by applying the fused sensor data to the HOSM observer for generating the states.

The paper is organised as follows: Section 2 describes the smart structure system used in this work and its mathematical model. Review of higher order sliding mode observer, measurement fusion and discrete sliding mode controller is presented in section 3. Design of observer and controller is presented in section 4. Simulation results are presented in section 5. Conclusions are given in section 6.

2. Smart structure system

The piezo actuated structure considered in this work is shown in Fig. 1. Two piezo ceramic patches, which act as sensors are bonded on the bottom surface of the beam, one at a distance of 10 mm and the other at a distance of 105 mm from the fixed end. Another pair of piezo patches are bonded on the top surface of the beam, one at a distance of 10 mm and the other at a distance of 375 mm from the fixed end, to act as control and disturbance actuators respectively.

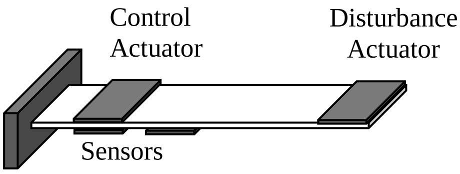

Fig. 1 Schematic of the piezo actuated structure

Table 1 Properties and dimensions of aluminium beam

Length (m)	0.45
Width (m)	0.0135
Thickness (m)	0.001
Young's modulus (Gpa)	71
Density (kg/m^3)	2700
First mode frequency (Hz)	5.5
Second mode frequency (Hz)	30.4

Table 2 Properties and dimensions of piezo ceramic sensor/ actuator

Length (m)	0.0765
Width (m)	0.0135
Thickness (m)	0.0005
Young's modulus (Gpa)	47.62
Density (kg/m^3)	7500
Piezoelectric strain constant (mV^{-1})	-247x10^{-12}
Piezoelectric stress constant (VmN^{-1})	-9x10^{-3}

Disturbance is applied to the structure through the disturbance actuator. The dimensions and properties of the aluminium beam and piezo ceramic sensor / actuator are given in Tables 1 and 2 respectively.

The linear time invariant continuous time, fourth order model of the smart structure reported in Arunshankar and Umapathy (2012) is considered in this work

$$\dot{x} = Ax + Bu + Er;\; y = Cx \tag{1}$$

$x \in \Re^n$, $u \in \Re^m$, $y \in \Re^p$, $E \in \Re^{nxq}$, $q \le p \le n$, with A the system matrix, B control input vector, E disturbance vector, C output matrix, x state vector, u controller output, and y controlled output.

$$A = \begin{bmatrix} 92.1084 & 64.5070 & -39.8911 & 65.1749 \\ -159.5286 & 14.3813 & 112.5734 & -118.4229 \\ 116.4182 & -111.6173 & -15.247 & 160.9807 \\ -63.1027 & 39.0227 & -63.7560 & -93.4438 \end{bmatrix}$$

$$B = \begin{bmatrix} -0.5220 \\ 0.2457 \\ -0.3766 \\ 0.7240 \end{bmatrix} \quad E = \begin{bmatrix} -0.0141 \\ -0.0387 \\ 0.0421 \\ 0.0058 \end{bmatrix} \quad C = \begin{bmatrix} 1 & 0 & 0 & 0 \end{bmatrix}$$

The discrete model of the above system, for a sampling interval of τ = 0.01 sec is

$$\begin{aligned} x(k+1) &= \Phi_\tau x(k) + \Gamma_\tau u(k) + E_\tau d(k) \\ y(k) &= C^T x(k) \end{aligned} \tag{2}$$

Where

$$\Phi_\tau = \begin{bmatrix} 1.2049 & 1 & 0 & 0 \\ -0.7429 & 0 & 1 & 0 \\ 1.1998 & 0 & 0 & 1 \\ -0.9782 & 0 & 0 & 0 \end{bmatrix}$$

$$\Gamma_\tau = \begin{bmatrix} -0.0042 \\ 0.0008 \\ -0.0014 \\ 0.0064 \end{bmatrix} \quad E_\tau = \begin{bmatrix} -0.00039 \\ 0.00060 \\ -0.00027 \\ 0.000019 \end{bmatrix}$$

$$C^T = \begin{bmatrix} 1 & 0 & 0 & 0 \end{bmatrix}$$

3. Review of HOSM observer, measurement fusion and controller

3.1 HOSM observer

For the smart structure system given in Eq. (1), the objective is to synthesize an observer to generate a state estimate $\hat{x}(t)$ and output estimate $\hat{y}(t) = C\hat{x}(t)$, such that a sliding mode is attained in which the output error

$$e_y(t) = \hat{y}(t) - y(t) \tag{3}$$

is forced to zero in finite time. The observer considered is of the form

$$\dot{\hat{x}}(t) = A\hat{x}(t) + Bu(t) - G_l e_y(t) + G_n v \tag{4}$$

With $G_l, G_n \in \Re^{nxp}$ are gain matrices and, v represents a discontinuous switching component to induce a sliding motion. The SMO of the form given in Eq. (4), which rejects the uncertainty will exist if and only if the nominal linear system, defined by the triple (A,E,C) satisfies the conditions rank(CE) = q, with the invariant zeros of the triple (A,E,C) must lie in $C\_$, the open left half of the complex plan. For a square system, where $p = q$, it should be noted that the above two conditions fundamentally require the triple (A,E,C) to be relative degree one and minimum phase. Under these assumptions, there exists a linear change of coordinates $x \mapsto Tx$ such that in the new coordinate system

$$\begin{aligned} \dot{x}_1(t) &= A_{11}x_1(t) + A_{12}x_2(t) + B_1 u(t) \\ \dot{x}_2(t) &= A_{21}x_1(t) + A_{22}x_2(t) + B_2 u(t) + Er \\ y(t) &= x_2(t) \end{aligned} \tag{5}$$

$x_1 \in \Re^{(n-p)}, x_2 \in \Re^p$ and the matrix A_{11} has stable eigen values. The coordinate system above will be used as a platform for the design of a SMO. For a dynamical system of the form

$$\begin{aligned}
&\dot{\hat{x}}_1(t) = A_{11}\hat{x}_1(t) + A_{12}\hat{x}_2(t) + B_1u(t) - A_{12}e_y(t) \\
&\dot{\hat{x}}_2(t) = A_{21}\hat{x}_1(t) + A_{22}\hat{x}_2(t) + B_2u(t) - (A_{22} - A_{22}^S)e_y(t) + v \\
&\hat{y}(t) = \hat{x}_2(t)
\end{aligned} \tag{6}$$

A_{22}^s is a stable design matrix, the discontinuous vector v is obtained from the super-twisting algorithm (STA) as reported in Rolink *et al.* (2006). If the state estimation errors are defined as $e_1 = \hat{x}_1 - x_1$ and $e_2 = \hat{x}_2 - x_2$ then

$$\begin{aligned}
&\dot{e}_1(t) = A_{11}e_1(t) \\
&\dot{e}_y(t) = A_{21}e_1(t) + A_{22}^S e_y(t) + v - \mathrm{Er}
\end{aligned} \tag{7}$$

Since in this situation $e_y = e_2$. The nonlinear error system given by Eq. (7) is quadratically stable and a sliding motion takes place forcing e_y=0 in finite time. The dynamical system given in Eq. (6) is thus regarded as an observer for the system given in Eq. (1). It follows that, after transformation of the system

$$G_l = T^{-1}\begin{bmatrix} A_{12} \\ A_{22} - A_{22}^s \end{bmatrix} \text{ and } G_n = T^{-1}\begin{bmatrix} 0 \\ I_p \end{bmatrix} \tag{8}$$

Hence the observer given in Eq. (6) can be written in terms of the original coordinates in the form of Eq. (4). STA depends only on the actual value of the sliding variable, and it is effective only for chattering attenuation purpose, as reported in Perruquetti and Barbot (2002), Pisano and Usai (2011). It however, does not require the output derivative to be measured, which makes it less complex, hence STA can be readily implemented in real time. As reported in Khan *et al.* (2003), STA has been originally developed and analysed for systems with relative degree one with respect to the input as in Eq. (9)

$$\dot{s} = \varphi(s,t) + \gamma(s,t)u \tag{9}$$

Where $0 < |\varphi(.)| \le \Phi$ and $0 < \Gamma_m \le \gamma(.) \le \Gamma_M$. STA defines the control law $u(t)$ as the combination of two terms, the first is defined by means of its discontinuous time derivative, and the second is a continuous function of the available sliding variable

$$\begin{aligned}
&u(t) = u_1(t) + u_2(t) \\
&\dot{u}_1(t) = \begin{cases} -u & \text{if } |u| > 1 \\ -W\mathrm{sign}(s) & \text{if } |u| \le 1 \end{cases} \\
&u_2(t) = \begin{cases} -\lambda|s_0|^\rho\,\mathrm{sign}(s) & \text{if } |s| > s_0 \\ -\lambda|s|^\rho\,\mathrm{sign}(s) & \text{if } |s| \le s_0 \end{cases}
\end{aligned} \tag{10}$$

Where $|S| < s_0$. The trajectories of the algorithm 'twist' around the origin in the phase portrait of the sliding variable, the corresponding sufficient conditions for the finite time convergence to the sliding manifold are

$$\begin{aligned}
&W > \frac{\Phi}{\Gamma_m} \\
&\lambda^2 \ge \frac{4\Phi}{\Gamma_m^2}\frac{\Gamma_M(W+\Phi)}{\Gamma_m(W-\Phi)} \\
&0 < \rho \le 0.5
\end{aligned} \tag{11}$$

The choice $\rho = 0.5$ ensures that the maximal possible 2-sliding realization for real sliding order two is achieved. This controller may be simplified when the controlled system is linearly dependent on control, u does not need to be bounded and $s_0 = \infty$

$$\begin{aligned}
&u = -\lambda|\sigma|^\rho\,\mathrm{sign}(s) + u_1 \\
&\dot{u}_1 = -W\mathrm{sign}(s)
\end{aligned} \tag{12}$$

3.2 Measurement fusion

In measurement fusion, output of the sensors is combined first and then this fused data is used to estimate the state vector, as reported in Roecker and McGillem (1998). Since the measurement noise is independent for sensors i and j, the equation for fusing the measurement vectors z_k^i and z_k^j, in recursive form, to obtain the minimum mean square estimate $\bar{z}_k$ is

$$\bar{z}_k = z_k^j + R_k^i(R_k^i + R_k^j)^{-1}(z_k^j - z_k^i) \tag{13}$$

Where R_k^i is the covariance matrix of the measurement vector z_k^i. These filtered measurements can then be tracked to obtain the estimate of the state vector $\hat{x}_{k/k}$, and has a covariance matrix

$$\bar{R}_k = [(R_k^i)^{-1} + (R_k^j)^{-1}]^{-1} \tag{14}$$

3.3 Discrete sliding mode controller

DSMC does not possess the invariance property found in continuous time sliding mode controller. The control input is constant during the sampling interval, hence when the states reach the switching surface, the controller would be unable to keep the states to be confined to the sliding surface. Thus the system undergoes only quasi-sliding mode, where the system states would approach the sliding surface, but would generally be unable to stay on it. Gao *et al.* (1995) introduced the 'reaching law' method to design the controller for continuous time system and extended the same for discrete time system. The switching function is effectively controlled to meet the required dynamics and also to satisfy the constraints of DSMC. This method is simple, since it directly deals with the reaching phase and obtaining the control law is easier. The reaching law based SMC for a discrete time system for a sampling interval $\tau > 0$ is

$$s(k+1) - s(k) = -q\tau s(k) - \varepsilon\tau sgn(s(k)) \tag{15}$$

With $\varepsilon > 0$, $q > 0$, $1 - q\tau > 0$, ε and q are gains named 'reaching speed' and 'index of reaching speed' respectively. The controller design involves the choice of these gain values. If ε is too small, the reaching time will be too long. On the other hand, larger value of ε will cause severe chattering. Also, due to the presence of the proportional rate term $-qs(t)$, the state is forced to approach the switching manifold faster when s is large. With the switching function

$$s(k) = c^T x(k) = 0 \tag{16}$$

The incremental change in $S(k)$ is

$$\begin{aligned} s(k+1) - s(k) &= c^T x(k+1) - c^T x(k) \\ &= c^T \Phi_\tau x(k) + c^T \Gamma_\tau u(k) - c^T x(k) \end{aligned} \tag{17}$$

Comparing it to the reaching law in Eq. (15)

$$\begin{aligned} s(k+1) - s(k) &= -q\tau s(k) - \varepsilon\tau sgn\big(s(k)\big) \\ &= c^T \Phi_\tau x(k) + c^T \Gamma_\tau u(k) - c^T x(k) \end{aligned} \tag{18}$$

Solving for $u(k)$ gives the control law

$$u(k) = Fx(k) + \gamma sgn(s(k)) \tag{19}$$

Where

$$F = -(c^T\Gamma_\tau)^{-1}[c^T\Phi_\tau - c^T I + q\tau c^T]$$

$$\gamma = -(c^T\Gamma_\tau)^{-1}\varepsilon\tau$$

For the system represented in controllable canonical form, the control law is given by

$$F_c = -(c^T\Gamma_{\tau,c})^{-1}[c^T\Phi_{\tau,c} - c^T I + q\tau c^T]$$

Solving for $u(k)$ gives the control law

$$u(k) = -(c^T\Gamma_\tau)^{-1}[c^T\Phi_\tau x(k) + \Gamma_\tau d(k) - c^T Ix(k) + q\tau c^T x(k) + \varepsilon\tau sgn(s(k))] \tag{20}$$

4. Observer and controller design

The piezo sensor output used for measuring the vibration of the smart structure considered are simulated, using the mathematical model of the structure, with the measurement noise covariances of the first and second sensor taken as 0.01 and 0.05 respectively. The HOSM observer is designed with λ=14, W=4 and ρ=0.5. The conventional observer designed for the discrete time model of the structure, with the desired eigen values taken as 0.3, 0.8, -0.3 and -0.8, resulted in the observer gain

$$Ke = \begin{bmatrix} 1.2049 \\ -1.4727 \\ 1.1998 \\ -0.9206 \end{bmatrix}$$

The discrete time model of the smart structure system is transformed to canonical form, and the weight matrices G_l and G_n associated with the HOSM observer obtained are

$$G_l = \begin{bmatrix} 1.0004 \\ -1.426 \\ 1.185 \\ -0.9758 \end{bmatrix} \qquad G_n = \begin{bmatrix} -0.0003906 \\ 0.0000604 \\ -0.0002699 \\ 0.0000193 \end{bmatrix}$$

The linear dynamical equation of the system during the sliding mode is

$$x(k+1) = [I - \Gamma_\tau(c^T\Gamma_\tau)^{-1}c^T]\Phi_\tau x(k)$$

The selection of switching function $c^T = [-0.045\ -0.255\ -0.05\ 1.0]$, $\varepsilon\tau = 0.001$, $q\tau = 0.01$ and $\tau = 0.01$ sec, gives the control law

$$u(k) = -[c^T\Phi_\tau x(k) - 0.0634d(k) - 0.99s(k) - 0.001sgn\big(s(k)\big)]$$

5. Simulation results

In the simulation carried out, the smart structure is excited at its first mode resonance, followed by the second mode resonance, using the disturbance actuator, for a duration of 5 seconds each, with the first and second mode frequencies being 5.5 Hz and 30.4 Hz respectively. The open loop response of the smart structure is given in Fig. 2.

The closed loop responses obtained with HOSM observer is shown in Fig. 3. The closed loop response of the structure obtained by using the states generated from the output of sensor I and the corresponding controller effort are given in Figs. 3(a) and 3(b) respectively.

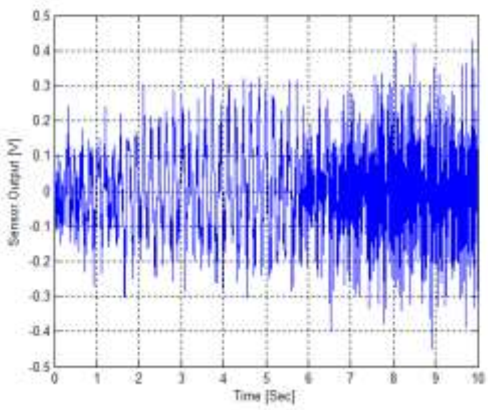

Fig. 2 Open loop response of smart structure system

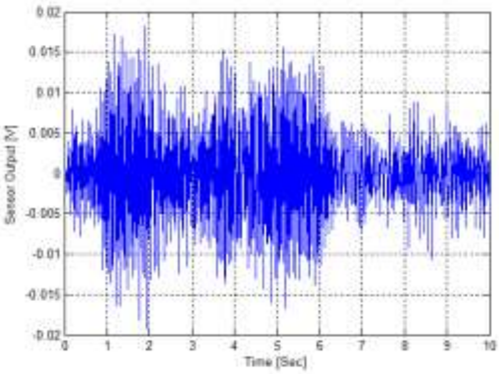

(a) Using states generated from output of Sensor I

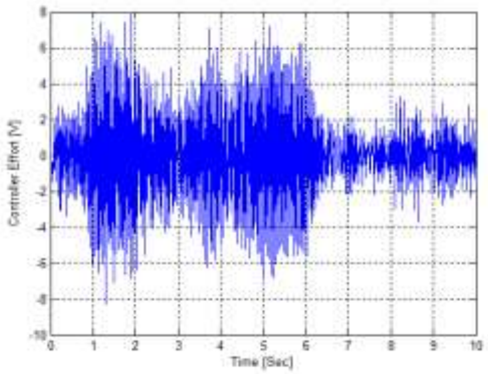

(b) Controller effort (Sensor I)

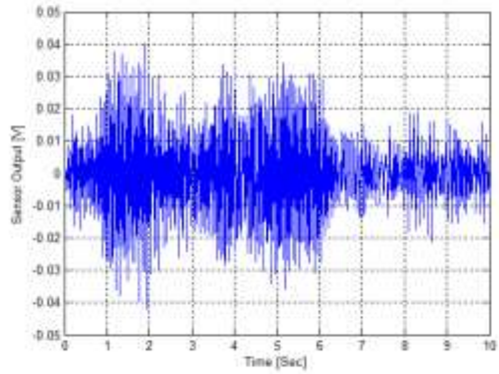

(c) Using states generated from output of Sensor II

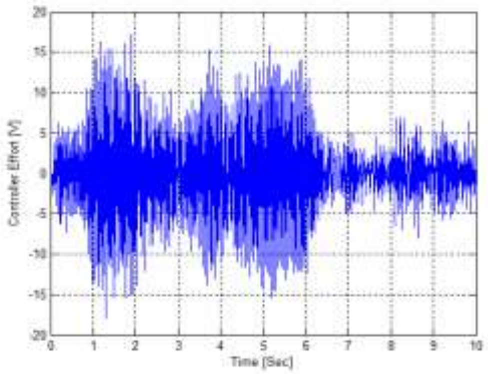

(d) Controller effort (Sensor II)

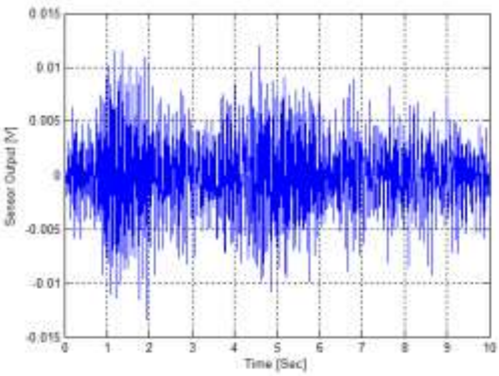

(e) Using states generated from fused output of Sensor I and Sensor II

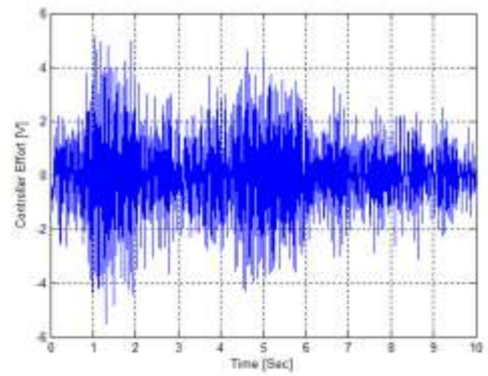

(f) Controller effort (Fused Data)

Fig. 3 Closed loop responses obtained with HOSM observer

The closed loop response of the structure obtained by using the states generated from the output of sensor II and the corresponding controller effort are given in Figs. 3(c) and 3(d) respectively. The closed loop response of the structure obtained by using the states generated from the fused output of sensor I and II, and the corresponding controller effort are given in Figs. 3(e) and 3(f) respectively.

The closed loop response obtained with conventional observer is shown in Fig. 4. The closed loop response of the structure obtained by using the states generated from the output of sensor I and the corresponding controller effort are given in Figs. 4(a) and 4(b) respectively. The closed loop response of the structure obtained by using the states generated from the output of sensor II and the corresponding controller effort are given in Figs. 4(c) and 4(d) respectively. The closed loop response of the structure obtained by using the states generated from the fused output of sensor I and II, and the corresponding controller effort are given in Figs. 4(e) and 4(f) respectively.

The performance indices ISE and IAE of the HOSM and conventional observer, with inputs from sensor I, sensor II, fused output of sensors I and II are given in Table 3. These indices show that the performance of both the observers is better, with input from sensor I, compared to their performance when the input are from sensor II, which is inline with the accuracy of the sensors taken in this work in terms of their measurement noise covariance.

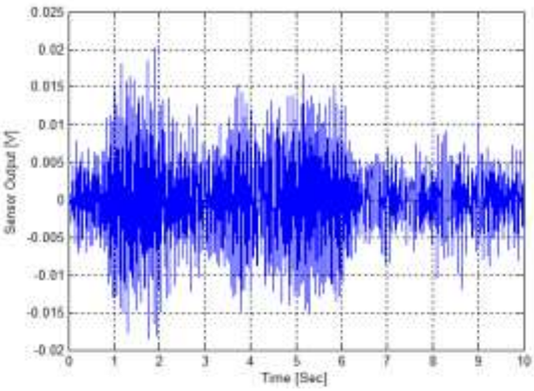

(a) Using states generated from output of Sensor I

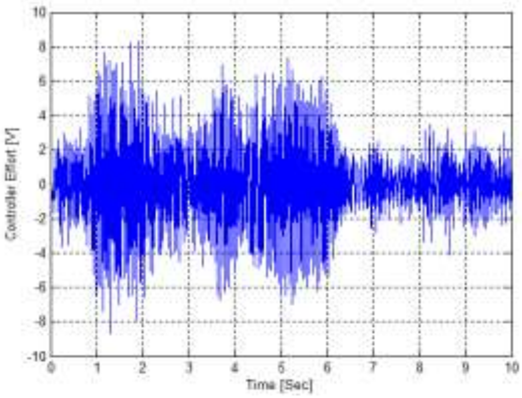

(b) Controller effort (Sensor I)

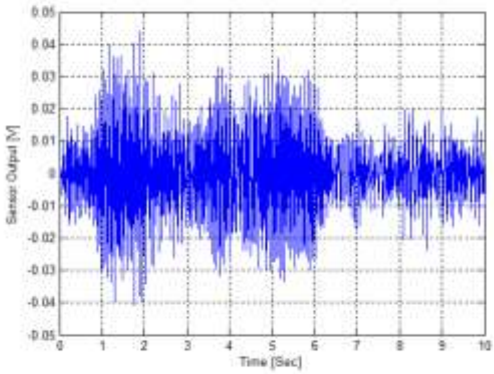

(c) Using states generated from output of Sensor II

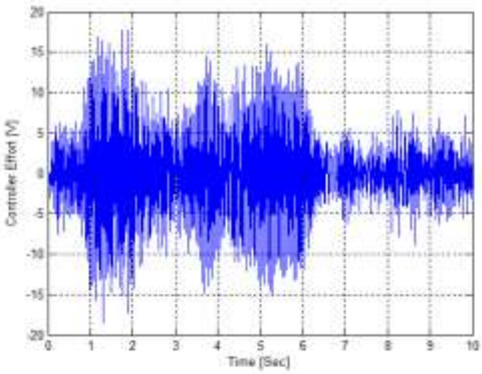

(d) Controller effort (Sensor II)

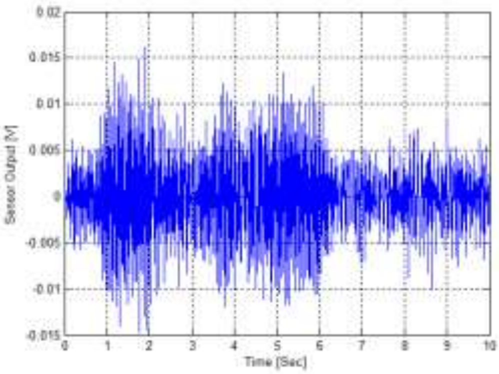

(e) Using states generated from fused output of Sensor I and Sensor II

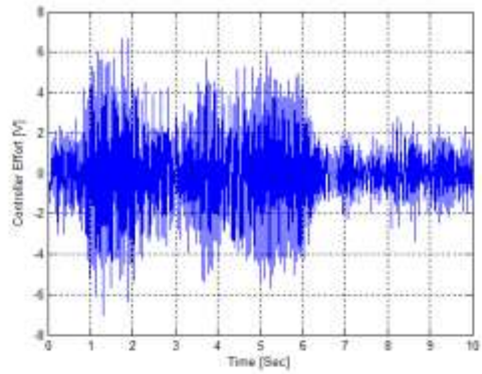

(f) Controller effort (Fused Data)

Fig. 4 Closed loop response obtained with conventional observer

Also the indices show that the performance of both the observers is better, with the fused output of sensors I and II are taken as input, compared to their performance with input taken from individual sensor. Hence application of data fusion has resulted in the improvement of observer performances.

The performance indices ISE and IAE of the controlled output, and the statistical specifications, the maximum value of the controlled output and the maximum controller output, obtained with HOSM observer and conventional observer being applied for closed loop control, are given in Tables 4 and 5 respectively. These indices show that, the closed loop response obtained using the states generated from sensor I data is better than the closed loop response obtained by using the states generated from sensor II data. Also the closed loop response obtained by using the states generated from fused data is better than the response obtained with the states generated from individual sensor data. The above improvement in the closed loop response propagates from the performances of the observers. The statistical specifications obtained also reflect the above results. It is evident to note that, the controller effort required to exercise control reduces, when the states generated by using the fused data of sensors is used as controller input. Also the closed loop response obtained with the states generated using HOSM observer is better than the closed loop response obtained with the states generated using conventional observer.

Table 3 Performance indices of HOSM observer and conventional observer

Observer Input	HOSM Observer Error		Conventional Observer Error	
	ISE, $(\text{Volts})^2$	IAE, Volts	ISE, $(\text{Volts})^2$	IAE, Volts
Sensor I	27.8443	136.5244	27.7668	136.3279
Sensor II	68.5397	209.3923	68.4517	209.3216
Fused Data of Sensor I & II	24.3319	128.8671	23.9740	127.9016

Table 4 Performance indices and statistical specifications of closed loop response obtained with HOSM observer

Controller Input	Performance Indices		Statistical Specifications	
	ISE of controlled output, $(\text{Volts})^2$	IAE of controlled output, Volts	Maximum controlled output, Volts	Maximum controller output, Volts
States generated from Sensor I	0.0398	5.0074	0.0182	7.8866
States generated from Sensor II	0.1942	11.0232	0.0402	17.1623
States generated from fused data	0.0175	3.3488	0.012	5.1165

Table 5 Performance indices and statistical specifications of closed loop response obtained with conventional observer

Controller Input	Performance Indices		Statistical Specifications	
	ISE of controlled output, $(\text{Volts})^2$	IAE of controlled output, Volts	Maximum controlled output, Volts	Maximum controller output, Volts
States generated from Sensor I	0.0423	5.2023	0.0201	8.2549
States generated from Sensor II	0.2060	11.4319	0.0440	17.7734
States generated from fused data	0.0271	4.1838	0.0162	6.6685

In the simulation work performed, the measurement noise covariances of the first and second sensor are taken as 0.01 and 0.05 respectively. This difference in the sensor is taken because, combining data from multiple inaccurate sensors does not provide a significant overall advantage. Also combining data from multiple highly accurate sensors does not provide a significant increase in inference accuracy.

This is the reason for higher values of ISE and IAE of controlled output, maximum controlled output and maximum controller output, seen against Sensor II in Tables 4 and 5. Whereas the above performance indices and statistical specifications is better for the “Fused Data” case, when compared with the individual sensors, including the more accurate sensor and less accurate sensor. This depicts the advantage of data fusion.

6. Conclusions

In this paper, vibration control of a piezo actuated structure using DSMC is addressed. From the simulation results, it is found that,

- Improvement in the performance of HOSM observer is obtained, when fused data of piezo sensors are applied to it for generating state estimates. These states generated when applied as controller input to the DSMC, resulted in the improved closed loop performance of the DSMC. This performance improvement is due to the information contribution from two sensors when fusion is performed.

- Also better vibration suppression is obtained when the states generated using HOSM observer is applied as controller input, when compared to the states generated by the conventional observer being applied as controller input.

References

Arunshankar, J., Umapathy, M. and Ezhilarasi, D. (2011), "Design and implementation of sliding mode controller with multisensor data fusion for the control of a piezo actuated structure", *Defense. Sci. J.*, **61**(4), 346-353.

Arunshankar, J., Umapathy, M. and Bandhopadhyay, B. (2013), "Experimental evaluation of discrete sliding mode controller for piezo actuated structure with multisensor data fusion", *Smart. Struct. Syst.*, **11**(6), 569-587. http://dx.doi.org/10.12989/sss.2013.11.6.569.

Arunshankar, J. and Umapathy, M. (2015), "Simultaneous stabilization of piezo actuated structures using fast output sampling control involving data fusion", *J. Vib. Eng. Technol.*, **3** (4), 369-382.

Arunshankar, J. and Umapathy, M. (2012), "Control of a piezo actuated structure using robust loop shaping controller with GPC based precompensator involving data fusion", *Int. J. Imag. Robot*, **8**(2), 85-100.

Bierman, G. and Belzer, M. (1985), "A decentralized square root information filter / smoother", *Proceedings of the 24th IEEE Conference on Decision and Control*, Florida, USA.

Capisani, L.M., Ferrara, A., Ferreira de Loza, A. and Fridman, L. M. (2012), "Manipulator fault diagnosis via higher order sliding-mode observers", *IEEE T. Ind. Electron.*, **59**(10), 3979-3986. DOI: 10.1109/TIE.2012.2189534.

Chalanga, A., Kamal, S., Fridman, L.M., Bandyopadhyay, B. and Moreno, J.A. (2016), "Implementation of super twisting control: super twisting and higher order sliding mode observer-based approaches", *IEEE T. Ind. Electron.*, **63**(6), 3677-3684. DOI: 10.1109/TIE.2016.2523913.

Edwards, C., Spurgeon, S.K. and Patton, R.J. (2000), "Sliding mode observers for fault detection and isolation", *Automatica*, **36**(4), 541-553. https://doi.org/10.1016/S0005-1098(99)00177-6.

Fisco, N.R. and Adeli, H. (2011), "Smart structures: Part I - active and semi-active control", *Scientia Iranica A*, **18**(3), 275-284. https://doi.org/10.1016/j.scient.2011.05.034.

Fridman, L. and Levant, A. (2002), *Sliding Mode Control in Engineering*, Marcel Dekker, USA.

Gan, Q. and Harris, C. (2001), "Comparison of two measurement fusion methods for Kalman filter based multi sensor data fusion", *IEEE T. Aerosp. Electron. Syst.*, **37**(1), 273-279. DOI: 10.1109/7.913685.

Gao, W., Wang, Y. and Homaifa, A. (1995), "Discrete-time variable structure control systems", *IEEE T. Ind. Electron.*, **42**(2), 117-122. DOI: 10.1109/41.370376.

Hassani, F.A., Payam, A.F. and Fathipour, M. (2010), "Design of a smart MEMS accelerometer using nonlinear control principles", *Smart. Struct. Syst.*, **6**(1), 1-16. http://dx.doi.org/10.12989/sss.2010.6.1.001.

Husek, P. (2016), "Adaptive sliding mode control with moving sliding surface", *Appl. Soft. Comput.*, **42**, 178-183. https://doi.org/10.1016/j.asoc.2016.01.009.

Hurlebaus, S. and Gaul, L. (2006), "Smart structure dynamics," *Mech. Syst. Signal. Pr.*, **20**(2), 255-281. https://doi.org/10.1016/j.ymssp.2005.08.025.

Khan, M.K., Spurgeon, S.K. and Levant, A. (2003), "Simple output-feedback 2-sliding controller for systems of relative degree two", *Proceedings of the European Control Conference*, Cambridge, UK.

Kim, K., Choi, J., Koo, G. and Sohn, H. (2016), "Dynamic displacement estimation by fusing biased high-sampling rate acceleration and low-sampling rate displacement measurements using two-stage Kalman estimator", *Smart. Struct. Syst.*, **17**(4), 647-667. http://dx.doi.org/10.12989/sss.2016.17.4.647.

Kim, B., Washington, G.N. and Yoon, H.S. (2013), "Active vibration suppression of a 1D piezoelectric bimorph structure using model predictive sliding mode control", *Smart. Struct. Syst.*, **11**(6), 623-635. http://dx.doi.org/10.12989/sss.2013.11.6.623.

Lei, Y., Luo, S. and Su, Y. (2016), "Data fusion based improved Kalman filter with unknown inputs and without collocated acceleration measurements", *Smart. Struct. Syst.*, **18**(3), 375-387. http://dx.doi.org/10.12989/sss.2016.18.3.375.

Li, L., Song, G. and Ou, J. (2013), "A nonlinear structural experiment platform with adjustable plastic hinges: analysis and vibration control", *Smart. Struct. Syst.*, **11**(3), 315-329. http://dx.doi.org/10.12989/sss.2013.11.3.315.

Liu, L., Zhu, J., Su, Y. and Lei, Y. (2016), "Improved Kalman filter with unknown inputs based on data fusion of partial acceleration and displacement measurements", *Smart. Struct. Syst.*, **17**(6), 903-915. http://dx.doi.org/10.12989/sss.2016.17.6.903.

Martin Liggins II, David Hall and James Llinas. (2008), *Handbook of multisensor data fusion: theory and practice*, (2nd Ed.), CRC Press, USA.

Mutambara, A.G.O. (1998), *Decentralized Estimation and Control for Multisensor Systems*, CRC Press, USA.

Nguyen, T., Su, W.C., Gajic, Z. and Edwards. C. (2016), "Higher accuracy output feedback sliding mode control of sampled data systems", *IEEE T. Ind. Electron.*, **63**(10), 3177-3182. DOI: 10.1109/TAC.2015.2505303

Palanisamy, R.P., Cho, S., Kim, H. and Sim, S.H. (2015), "Experimental validation of Kalman filter-based strain estimation in structures subjected to non-zero mean input", *Smart. Struct. Syst.*, **15** (2), 489-503. http://dx.doi.org/10.12989/sss.2015.15.2.489.

Perruquetti, W. and Barbot, J. P. (2002), *Sliding Mode Control in Engineering*, Marcel Dekker, USA.

Pisano, A. and Usai, E. (2011), "Sliding mode control: a survey with applications in math", *Math. Comput. Simulat.*, **81**(5), 954-979. https://doi.org/10.1016/j.matcom.2010.10.003.

Roecker, J.A. and McGillem, C.D. (1998), "Comparison of two-sensor tracking methods based on state vector fusion and measurement fusion", *IEEE T. Aerosp. Electron. Syst.*, **24**(4), 447-449. DOI: 10.1109/7.7186.

Rolink, M., Boukhobza, T. and Sauter, D. (2006), "High order sliding mode observer for fault actuator estimation and its application to the three tanks benchmark", *Workshop on Advanced Control and Diagnosis*, Nancy, France.

Utkin, V.I. (1992), *Sliding Modes in Control and Optimization*, Springer-Verlag, Germany.

Wang, H., Man, Z., Kong, H., Zhao, Y., Yu, M., Cao, Z., Zheng, J. and Do, M.T. (2016), "Design and implementation of adaptive terminal sliding mode control on a steer-by-wire equipped road vehicle", *IEEE T. Ind. Electron.*, **63**(9), 5774-5785. DOI: 10.1109/TIE.2016.2573239.

Xu, Q. (2017), “Precision motion control of piezoelectric nanopositioning stage with chattering free adaptive sliding mode control”, *IEEE T. Autom. Sci. Eng.*, **14**(1), 238-248. DOI: 10.1109/TASE.2016.2575845.

Xu, R. and Zhou, M. (2017), “Sliding mode control with sigmoid function for the motion tracking control of the piezo actuated stages”, *Electron. Lett.*, **53**(2), 75-77. DOI: 10.1049/el.2016.3558.

Zhang, J., Liu, X., Xia, Y., Zuo, Z. and Wang, Y. (2016), “Disturbance observer based integral sliding mode control for systems with mismatched disturbances”, *IEEE T. Ind. Electron.*, **63**(11), 7040-7048. DOI: 10.1109/TIE.2016.2583999.

Zhao, L., Huang, J., Liu, H., Li, B. and Kong, W. (2014), “Second order sliding-mode observer with online parameter identification for sensorless induction motor drives”, *IEEE Trans. Ind. Electron.*, **61**(10), 5280-5289. DOI: 10.1109/TIE.2014.2301730.

HJ